JOURNAL OF
MOLECULAR
CATALYSIS
A: CHEMICAL

Autocatalytic formation of colloidal mercury in the redox reaction between Hg^{2+} and Fe^{2+} and between Hg_2^{2+} and Fe^{2+}

Raquel R. Raposo [a,*], Enrique Meléndez-Hevia [b], Michael Spiro [c]

[a] *Universidad de La Laguna, Departamento de Química Física, Facultad de Farmacia, Tenerife 38206, Canary Islands, Spain*
[b] *Universidad de La Laguna, Departamento de Bioquímica, Edificio Central, Avda. Trinidad 59,*
La Laguna 38204, Tenerife, Canary Islands, Spain
[c] *Imperial College of Science, Technology and Medicine, Department of Chemistry, South Kensington, London SW7 2AY, UK*

Abstract

The reaction in perchloric acid solution between Hg^{2+} and Fe^{2+} was found to proceed extremely slowly until it suddenly exhibited an autocatalytic surge. In conjunction with this rise, a yellow-green by-product formed and disappeared again when the reaction came to an end. In the related reaction between Hg_2^{2+} and Fe^{2+}, the autocatalytic behaviour started early and the yellow-green by-product again appeared. No metallic mercury or other solid formed in either reaction, but the production of colloidal mercury was demonstrated by the Tyndall effect and by electrophoresis experiments. A five-step mechanism for these reactions is proposed and incorporated into a computer simulation called *Mercury*. The behaviour predicted by these simulations agrees well with the unusual experimental findings. © 2000 Elsevier Science B.V. All rights reserved.

Keywords: Iron(II); Mercury(I); Mercury(II); Mercury colloid; Autocatalysis; Computer simulation

1. Introduction

The only information on kinetics of the reaction between Hg^{2+} and Fe^{2+} in perchloric acid comes from two short reports by Adamson [1,2]. He explained the slowness of the reaction as due to the diamagnetism of Hg(II) and the high paramagnetism of Fe(II): in addition, of course, there will be electrostatic repulsion between the two cations. However, the half-life mentioned in the first report [1] is some three powers of 10 shorter than that calculated from the second order rate constants given in the second report [2]. It was also assumed that the Hg(II) would only be reduced to Hg(I) although some early 19th century workers reported reduction to metallic mercury in nitric acid

and in sulfuric acid media [3]. On reinvestigating this reaction, we discovered that the kinetics was quite unusual: an extremely rapid autocatalysis stage following a long inductive or feeding phase, sometimes with an initial hump in it, and we observed the temporary appearance of a coloured by-product. Detailed experimentation over a wide range of concentrations and temperatures, supported by computer simulation, has now revealed a complicated mechanism which involves the formation of colloidal metallic mercury.

2. Experimental

$Hg(NO_3)_2 \cdot H_2O$, $Hg_2(NO_3)_2 \cdot 2H_2O$, $Fe(ClO_4)_2 \cdot 6H_2O$, $Fe(NO_3)_3 \cdot 9H_2O$ and NaSCN were purchased from BDH/Merck, Johnson Matthey and Aldrich. Seventy percent $HClO_4$ came from Merck; KI and 35%

* Corresponding author.

HCl from Panreac (Barcelona, Spain). All products were AnalaR or analytical grade. Two different reactions were studied under several conditions: Reaction A ($Hg^{2+}+Fe^{2+}$) and Reaction B ($Hg_2^{2+}+Fe^{2+}$). Both reactions were carried out in 1 M $HClO_4$ to avoid hydrolysis of the reactant and product ions. They were followed either with a Perkin-Elmer Lambda 2 UV/Vis or with a GBC UV/Vis 918 Spectrophotometer (Dandenong, Australia). The second instrument included a peltier device for temperature control, and a carriage for six cells allowing us to follow several reactions simultaneously. The experiments were carried out over the range 20–90°C. This system also allowed us to obtain a continuous recording of the reaction progress at different wavelengths at the same time. Reactions were carried out in quartz cells (Sigma C-9417), which have no absorbance from 200 nm. Total volume of the reactions was generally about 3 ml. In some runs, the reaction was also followed with the addition of sodium thiocyanide to check the production of the red complex, $FeSCN^{2+}$, at 460 nm [4]. The presence of the dimeric mercurous ions was tested with 12 M HCl (which gives a white precipitate of Hg_2Cl_2) [5] and the presence of Hg^{2+} with potassium iodide (which gives a red precipitate) [6].

Preliminary experiments showed that this reaction is extremely slow, both at low reagent concentrations and at normal temperatures. For example, at 1 mM of each reagent and 80°C, the reaction took 4 days to come to completion: when the concentration of each reagent was 50 mM and the temperature 25°C, the reaction took ca. 1 week. Thus, in order to work with convenient times, we generally employed a high concentration range of Fe^{2+} and Hg^{2+} between 25 and 100 mM, and temperatures between 30°C and 60°C; under these conditions, the total reaction was completed between 30 min and several hours.

In some experiments, the reaction was monitored at the Fe^{3+} peak of 250 nm [7]. However, in most experiments, Fe^{3+} was monitored at 330 nm (extinction coefficient at this wavelength: 18.5 M^{-1} cm^{-1}) which is better for high concentrations, and avoids a possible overlap with the very high absorbance of Hg_2^{2+} whose maximum is at 236 nm, or with other possible species, such as Hg^+ which has a maximum at 272 nm [8]. The reaction was also followed at 450 nm to see the kinetics of the yellow-green by-product (Fig. 1). The effect of oxygen on the reaction was negligible; no
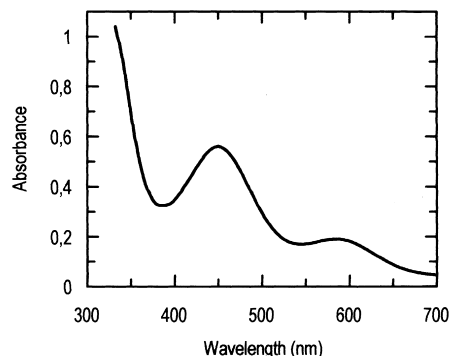

Fig. 1. Absorption spectrum of the by-product. A coloured form of the colloidal mercury produced in the whole reaction with 50 mM Fe^{2+} and 50 mM Hg^{2+} at 45°C. Apart from Fe^{3+} (whose extinction coefficient is 18.49 M^{-1} cm^{-1} at 330 nm, and 3.817 M^{-1} cm^{-1} at 250 nm) [7], no other reactant species absorbs significantly in this range.

difference was noticed between reactions carried out normally and under a nitrogen atmosphere.

Electrophoresis was used to investigate the presence of the colloidal metallic mercury in the product of the reactions. Reaction A was run with 50 mM of each reagent and, at the end, the remaining Hg^{2+} was eliminated with successive precipitations with 1 M KI and centrifuged. A similar process was also carried out with the product of Reaction B run with 50 mM Fe^{2+} and 25 mM Hg_2^{2+}, removing the excess of the mercurous reagent by successive precipitations with 1 M HCl and centrifuging. Electrophoresis was carried out with platinum wire electrodes polished with Al_2O_3. It was continued for several hours at 1.5 V until enough of the product had been seen on the electrodes.

3. Results and discussion

3.1. Reaction A between Hg^{2+} and Fe^{2+}

Progress curves of Reaction A under different conditions are plotted in Figs. 2 and 3. Instead of the typical kinetic curve of a reaction, with decreasing slope as it approaches equilibrium, the progress curve of this system showed a long first induction or feeding stage followed by a rapid autocatalytic rise in rate. We shall take the long following horizontal absorbance at 330 or 250 nm as indicating the end of the reaction.
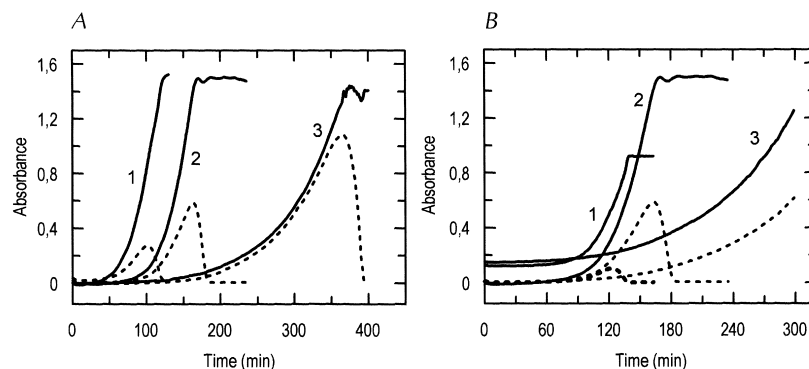
Fig. 2. Typical progress curves of Reaction A (between Hg^{2+} and Fe^{2+}). Effect of the ratio of Fe^{2+}/Hg^{2+} on the reaction rate at 45°C in 1 M perchloric acid. Full lines: Fe^{3+} progress recorded at 330 nm; dashed lines: progress of the yellow-green by-product recorded at 450 nm. (A) Experiments at constant Fe^{2+} (50 mM) and variable Hg^{2+} (1, 100 mM; 2, 50 mM; 3, 25 mM). Here the reaction rate is lower with decreasing Hg^{2+} concentration, and more by-product is formed. (B) Experiments at constant Hg^{2+} (50 mM) and variable Fe^{2+} (1, 25 mM; 2, 50 mM; 3, 100 mM). Here the increase of Fe^{2+} slows the reaction down, and the amount of the by-product increases markedly.

When the reaction was carried out at high concentrations of the reagents (of the order 50 mM), a point was reached at which the solution turned a yellow-green colour which has an absorbance maximum at 450 nm (Fig. 1). This was due to a by-product which formed and increased during the acceleration stage of the reaction and became depleted at the end. At low r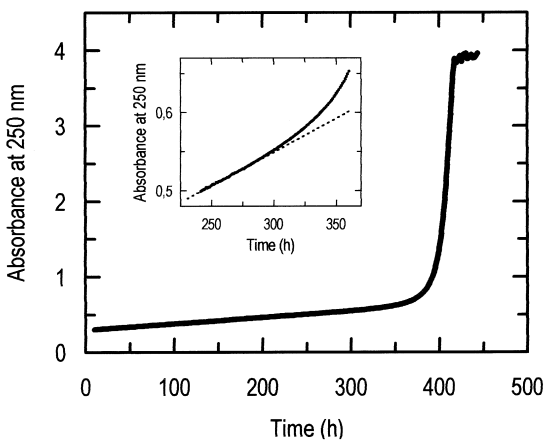eactant concentrations (of the order 1 mM), the induction period lasted for hundreds of hours and no colour change was seen (Fig. 3).

The reaction yielded Fe^{3+} as demonstrated by its absorption spectrum and by the red complex formed on adding thiocyanide. No Hg_2^{2+} was detected at the end of the reaction with the HCl test, nor was any grey precipitate of metallic mercury ever observed. This suggests that the mercury product was stabilised in a colloidal form that we designated Hg_c^0. Mercury sols are well known [9] and evidence for their formation is given below.

3.2. Reaction B between Hg_2^{2+} and Fe^{2+}

Since Reaction A is likely to proceed via an Hg^+ intermediate, and since Hg^+ can rapidly dimerise in homogeneous solution [8], the related Reaction B:

$$\frac{1}{2}Hg_2^{2+} + Fe^{2+} \rightarrow Hg^0 + Fe^{3+}, \tag{B}$$
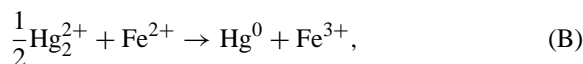
provides useful insight into the mechanism of Reaction A. The literature states that Reaction B is very slow [10]. Our experiments confirmed that it was very slow at low concentrations (3–10 mM of each reagent). However, at high concentrations (around 50 mM Fe^{2+} and 25 mM Hg_2^{2+}), a marked autocatalytic effect was observed which has not been mentioned in the literature. A typical example is shown in Fig. 4. However, unlike the autocatalysis exhibited by Reaction A
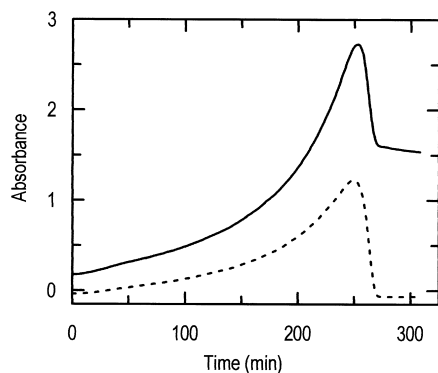

Fig. 3. Kinetic curve of Reaction A (between Hg^{2+} and Fe^{2+}) of a typical experiment at low concentrations (1 mM each, in 1 M perchloric acid) at 80°C, recorded at 250 nm. The by-product is not apparent under these conditions, and the linear stage is very long. The inset shows the last part of that stage, and the explosive triggering to the exponential phase.

Fig. 4. Reaction B (between Hg_2^{2+} and Fe^{2+}) carried out with 25 mM of mercurous nitrate and 50 mM of ferrous perchlorate in 1 M perchloric acid at 45°C, recorded at 330 nm to see the Fe^{3+} progress (full line) and at 450 nm to see the by-product (dashed line).

in Fig. 2, here it started near the beginning, without a feeding stage. The logical candidate for this auto-catalysis is colloidal metallic mercury since metallic surfaces catalyse many redox reactions [11] and so do colloidal metals [12]. No precipitate of metallic mercury was ever observed. On the other hand, the yellow-green by-product was again seen. Fig. 4 shows that it reached a relatively higher concentration than in Reaction A.

3.3. Colloid production

The results suggest that in both reactions, two forms of colloid are produced: a colourless form which remains at the end of the reaction, and the yellow-green by-product which is suddenly depleted at the end. The presence of colloidal mercury was demonstrated experimentally by means of the Tyndall effect (Fig. 5). These photographs also show the Brownian movement [13] of the particles.

Evidence for colloid formation in Reaction B was also obtained by electrophoresis. As Fig. 6B shows, a deposit of small spheres of metallic mercury attached to the cathode could be seen under the microscope and even by direct observation. The colloid had clearly been stabilised by cation adsorption since it was deposited on the cathode. For Reaction A, however, electrophoresis yielded scarcely visible balls of metallic mercury, surrounded by an abundant and diverse precipitate on the cathode, which made it hard to see them (Fig. 6A).

In Reaction A, the yellow-green colour was only formed at high amounts of Fe^{2+}, and was enhanced with iron concentration. Since it appeared as the reaction progressed (Fig. 2), it is likely to be a special form of colloidal mercury with Fe^{2+} attached as a colloid stabiliser. This could explain the disappearance of the coloured by-product at the end of the process because
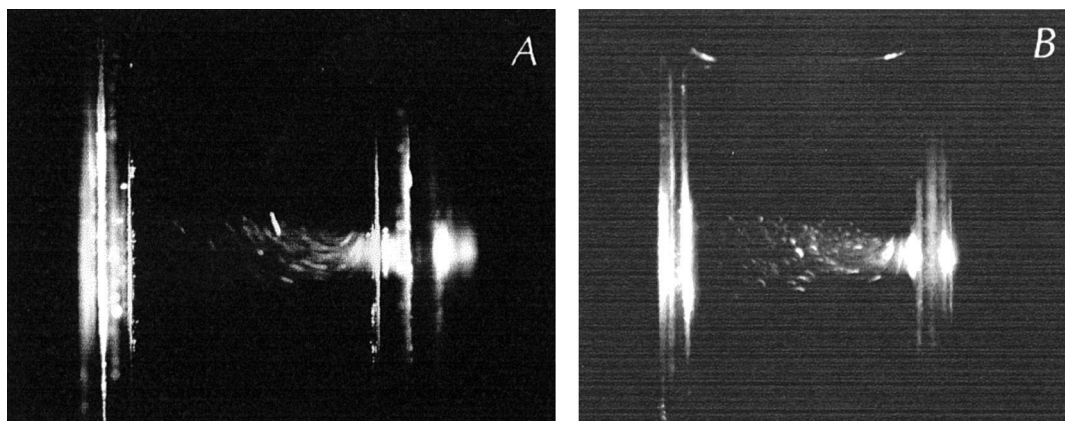

Fig. 5. The Tyndall effect which demonstrates the colloidal metallic mercury as a product of the reactions. Glass cuvettes of $2.5 \times 2.5 \times 7.0$ cm³, with 30 ml of reaction mixtures illuminated with a halogen lamp of 220 V and 50 W, with a lampshade device to provide a thin light beam. (A) Product of the whole reaction (Reaction A) carried out with 1 mM Fe^{2+} and 5 mM Hg^{2+}. (B) Product of Reaction B carried out with 50 mM Fe^{2+} and 25 mM Hg_2^{2+}; 100 ASA Kodak film was used with diaphragm 8. These photographs were taken with long exposure (5 s in A, and 3 s in B), which allows observation of the trajectory of the particles typical of the Brownian movement.
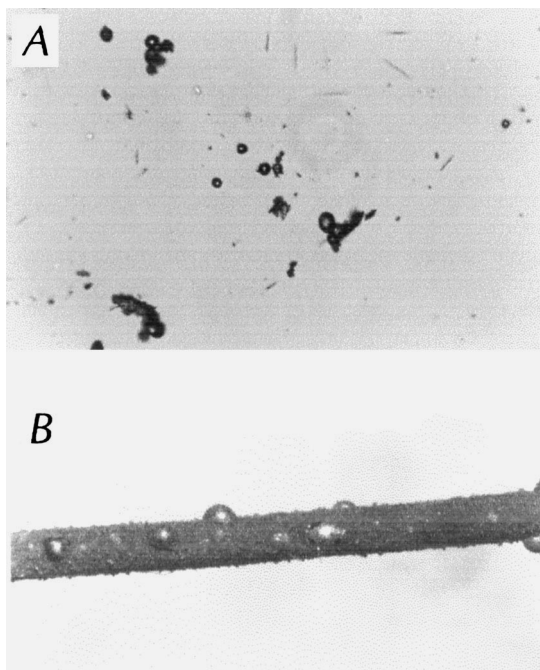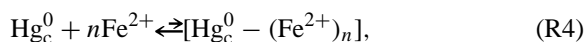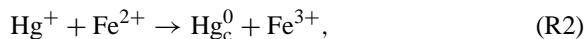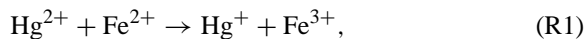
Fig. 6. Deposits of metallic mercury obtained by electrophoresis of the reaction products. Photographs from microscope images. (A) Small spheres of metallic mercury, as produced by Reaction A carried out with 10 mM Hg^{2+} and 20 mM Fe^{2+}. Magnification: ×200. Before electrophoresis, the excess of the reagent Hg^{2+} was removed by precipitation with KI to avoid a spurious deposit of Hg by electrolysis. (B) Small spheres of metallic mercury attached to the cathode, as produced by Reaction B carried out with 25 mM Hg_2^{2+} and 50 mM Fe^{2+}. Magnification: ×25. Before electrophoresis, the excess of the reagent Hg_2^{2+} was removed by precipitation with HCl to avoid a spurious deposit of mercury by electrolysis.

the Fe^{2+} has been oxidised to Fe^{3+} whose stronger hydration shell would reduce its attachment. In fact, when the initial Fe^{2+} concentration was much higher than Hg^{2+}, some by-product would have still remained at the end. Moreover, if the reaction was run at moderately low Fe^{2+} concentrations, so that the colour was lost at the end, then a further addition of Fe^{2+} restored the colour and the absorbance at 450 nm, consistent with colloidal metallic mercury remaining at the end of the reaction.

3.4. Mechanistic model for Reaction A

We propose that the mercuric ion Hg^{2+} is successively reduced to Hg^+ and Hg^0 by Fe^{2+}. However,

our observations show that the metallic mercury produced is stabilised in colloidal form (Hg_c^0), and can react with Hg^{2+} to give $2Hg^+$ or be sequestered by Fe^{2+} to give the yellow-green by-product. This leads to the following five reactions:

$$Hg^{2+} + Fe^{2+} \rightarrow Hg^+ + Fe^{3+}, \tag{R1}$$

$$Hg^+ + Fe^{2+} \rightarrow Hg_c^0 + Fe^{3+}, \tag{R2}$$

$$Hg^{2+} + Hg_c^0 \rightarrow 2Hg^+, \tag{R3}$$

$$Hg_c^0 + nFe^{2+} \rightleftarrows [Hg_c^0 - (Fe^{2+})_n], \tag{R4}$$

$$2Hg^+ \rightleftarrows Hg_2^{2+}. \tag{R5}$$

This process is autocatalytic, since the product Hg_c^0 formed from 1 mol Hg^+ in Reaction R2 then reacts in its turn with new Hg^{2+} to yield 2 mol Hg^+ in R3. This produces a chain reaction, as other cases described in the literature [14] which continues to amplify the whole process while there are enough Hg^{2+} and Fe^{2+} ions. Reaction R4, however, acts as a brake by driving Hg_c^0 into the cul de sac by-product. The model is illustrated in Fig. 7. The mechanism is described by the following set of differential rate equations:

$$\frac{dFe^{3+}}{dt} = v_1 + v_2, \tag{1}$$

$$\frac{dHg^+}{dt} = v_1 - v_2 + 2v_3 - 2v_5, \tag{2}$$

$$\frac{dHg_c^0}{dt} = v_2 - v_3 - v_4, \tag{3}$$

$$\frac{dHg_{c-ByP}^0}{dt} = v_4, \tag{4}$$

$$\frac{dHg_2^{2+}}{dt} = v_5, \tag{5}$$

and the conservation equation:

$$Fe^{2+} = (Fe^{2+})_{t=0} - Fe^{3+} - nHg_{c-ByP}^0. \tag{6}$$

The various rates are given by:

$$v_1 = k_1Fe^{2+}Hg^{2+} - k_{-1}Fe^{3+}Hg^+, \tag{7}$$

$$v_2 = (k_2Fe^{2+}Hg^+)(1 + qHg_c^0) - k_{-2}Fe^{3+}Hg_c^0, \tag{8}$$

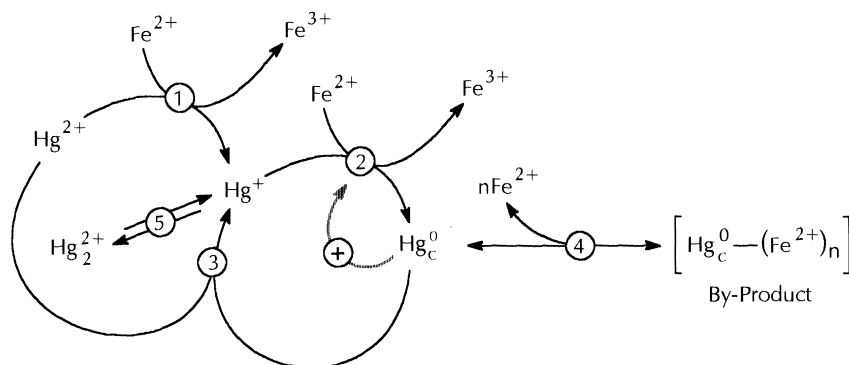$$v_3 = k_3Hg^{2+}Hg_c^0 - k_{-3}(Hg^+)^2, \tag{9}$$

Fig. 7. Model of the mechanism proposed for the global reaction between Hg^{2+} and Fe^{2+}. The whole process includes five different reactions, the formation of metallic colloidal mercury (Hg_c^0), and the activation by surface catalysis of that colloid on Reaction R2, represented in the scheme by the (+) arrow. Reactions R1 and R2 are conventional redox reactions between iron and mercury. Reaction R3 is the reverse dismutation of mercurous ion, and the other two reactions turn aside the intermediates from the global mechanism: Reaction R4 is the formation of a yellow-green colloid with an absorbance maximum at 450 nm, which we have named *by-product*, due to the cul de sac role in the global mechanism, and Reaction R5 is the dimerization of Hg^+. The stoichiometric coefficients have been omitted in this scheme, because they change in each cycle. The stoichiometry of Reaction R4 is indeterminate, and it could involve more cations in addition to Fe^{2+}. The set of Reactions R2 and R3 produces a kinetic autocatalysis cycle (chain reaction), as it duplicates the concentration of the intermediate Hg^+ in each turn. This effect is amplified by surface catalysis on Reaction R2. The role of Reaction R1 is only to feed the system, supplying Hg^+ until the autocatalysis is triggered.

$$v_4 = k_4 Hg_c^0 (Fe^{2+})^m - k_{-4} Hg_{c\text{-}ByP}^0, \qquad (10)$$

$$v_5 = k_5 (Hg^+)^2 - k_{-5} Hg_2^{2+}. \qquad (11)$$

The parameter q in Eq. 8 allows for the catalysis of the Reaction R2 by the colloidal mercury in a simplified form because the sizes and hence, the surface areas of the sol particles, are not known. The reaction must therefore be viewed as a complex network instead of a sequential number of steps [15].

A computer program called *Mercury* was then designed to simulate the general kinetic behaviour of this system. Numerical integration of kinetic equations was calculated by means of the Euler algorithm. *Mercury* was developed in Quick Basic v 4.5 [16] and run in a Pentium IBM PC compatible computer with 64 Mb RAM. A copy of Mercury in diskette is available on request.

By adjusting the parameters, *Mercury* allowed us to obtain simulated kinetics ("experiments in numero" [17]) which represented well the main features of the mechanism, namely the induction (feeding) phase, the explosive autocatalysis, and the formation and depletion of the by-product. This is shown in Fig. 8. The differences between the observed absorbances and the simulated absorbances calculated for the Fe^{3+} con-
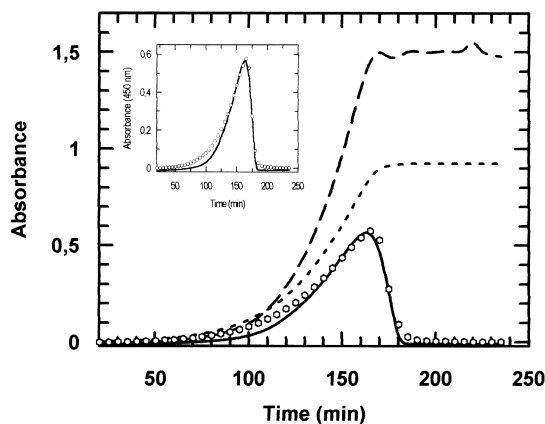

Fig. 8. Progress curves obtained by computer simulation, compared with experimental results of the reaction with 50 mM Hg^{2+} and 50 mM Fe^{2+} at 45°C. Dashed line: experimental curve of Fe^{3+} at 330 nm; dotted line: progress curve of Fe^{3+} simulated by computer; full line: experimental curve of the by-product, at 450 nm; open points: progress of the by-product simulated by computer; the kinetics of the by-product (experimental and simulated) is shown with more detail in the inset. The absorption of the colloid at 330 nm provokes the difference of absorbance of Fe^{3+} between experimental and simulated results.
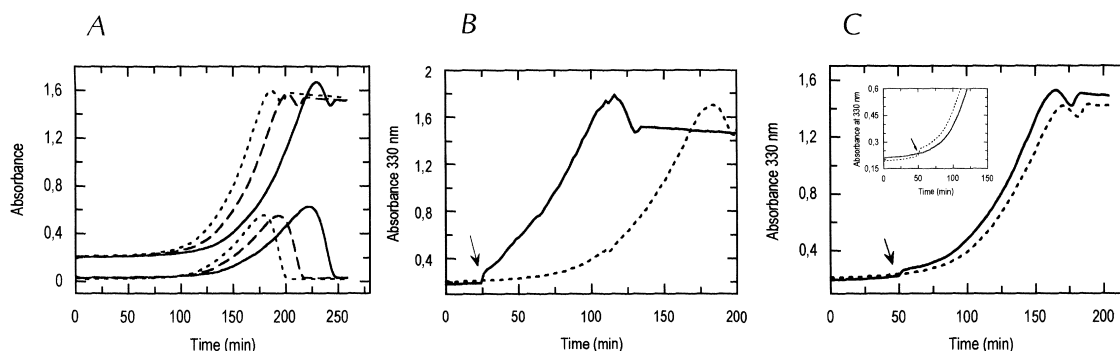
Fig. 9. Effect on the autocatalysis of adding different external mercury sources. (A) Small reductions of the feeding stage on adding Hg_2^{2+} at the start of 50 mM Fe^{2+} and 50 mM Hg^{2+} runs. Upper curves: Fe^{3+} recorded at 330 nm; lower curves: by-product recorded at 450 nm. Additions to the initial reaction: (—) none; (---) 2.5 mM $Hg_2(NO_3)_2$; ($\cdots$) 5 mM $Hg_2(NO_3)_2$ as final concentrations. (B) A great acceleration on adding the product of Reaction B (carried out with 50 mM Fe^{2+} and 25 mM Hg_2^{2+}). ($\cdots$) Control; (—) reaction where 50 μl of the product was added at the time indicated by the arrow. (C) Little effect on adding the same amount of the product of Reaction B when the autocatalytic phase had already started; symbols as in (B). Temperature was 45°C in all these experiments.

centrations are due to the absorbances of the mercury colloid [9]. To fit the experimental absorbances for the by-product, m (Eq. 10) was taken as 0.2, n (Eq. 6) was taken as 10, and its extinction coefficient was taken as 5000 $M^{-1}cm^{-1}$. Two different reverse rate constants k_{-41} and k_{-42} for the ascent and descent were needed to account for the peculiar observed peak of the by-product. This may be due to a gradual change in its composition.

Combination of these computer simulations and laboratory results led to the following relationships between the rate constants:

$$k_5 \geq k_2 > k_3 > k_4 > k_1 \text{ and } k_{-42} > k_{-41}. \tag{12}$$

The in numero calculations with *Mercury* revealed that, for the autocatalytic process to occur, k_5 must be much smaller than the diffusion-controlled rate constant for the dimerization of free Hg^+ ions [8]; this suggests that the ions Hg^+ are attached to and stabilise the colloidal mercury species.

The computer calculations also revealed that the induction period is not a true straight line but a curve with a very slow ascent which is difficult to detect experimentally (see the inset of Fig. 3). The lower k_1 and/or k_2, the slower and the longer is such a stage and so it is more difficult to appreciate its curvature. This stage is essentially in a quasi-stationary state. The values of the parameters and initial conditions for the case presented in Fig. 8 are shown in Appendix A.

3.5. The key intermediate

To find out which of the two intermediates, Hg^+ or Hg_c^0, in the proposed mechanism is the key one which triggers the autocatalysis, a *small amount* of each was added to Reaction A during the feeding phase. As Fig. 9A shows, small additions of $Hg_2(NO_3)_2$ scarcely, decreased the length of the feeding stage, and it was necessary to add a large amount (25 mM) to obtain a high response (see Table 1). In contrast, addition of a small volume (50 μl) of the product of Reaction B to Reaction A during the feeding stage produced an explosive triggering of autocatalysis (Fig. 9B). No such effect appeared when the same mixture was added when the autocatalytic phase had already started (Fig. 9C).

According to the model, there is competition for Hg_c^0 between the reactants, Hg^{2+} in Reaction R3 and Fe^{2+} in Reaction R4. The former leads to the autocatalysis while the latter just produces by-product. This explains the observed trends in Fig. 2 where a high Hg^{2+}/Fe^{2+} ratio increased the reaction rate (Fig. 2A), while a low Hg^{2+}/Fe^{2+} ratio had the opposite effect, with large by-product accumulation (Fig. 2B).

3.6. The critical mass

The experiments above suggest that the quasi-steady state induction period is needed to build up a criti-

Table 1

Effect of addition of the mercurous ion on the feeding time

In a series of experiments with 50 mM each of Fe^{2+} and Hg^{2+} at 45°C, different amounts of mercurous ion were added from the beginning. As a reference point, the maximum absorbance reached at 450 nm in Reaction B (25 mM Hg_2^{2+} + 50 mM Fe^{2+}) was 1.62.

Hg_2^{2+} (mM)	Time moved forward (min)	% Decrease of feeding phase	Maximum by-product absorbance	Critical mass $[Hg^{2+}] \cdot [\text{by-product}]$
0	0	0	0.60	30.0
0.25	10	5.9	0.75	37.5
5.0	30	13.0	0.55	27.5
10.0	42	18.3	0.55	27.5
25.0	72	42.3	0.50	25.0

cal mass of the key intermediate Hg_c^0. The reason is that sequestration of Hg_c^0 by Fe^{2+} allows the Hg_c^0 necessary for Reaction R3 to increase only very slowly. Moreover, the proportion of by-product to Hg_c^0 should be constant for a given Fe^{2+} concentration. Hence, at constant Fe^{2+} concentration, the absorbance of the by-product is an indirect measure of the Hg_c^0 available to Reaction R3. Table 1 shows that the maximum absorbance of the by-product remained constant when the reaction was accelerated with Hg_2^0 additions.

Since Reaction R3 is bimolecular, an increase of Hg^{2+} should compensate for a Hg_c^0 deficiency. The critical mass is thus related to a certain value of the concentration product $[Hg^{2+}] \cdot [Hg_c^0]$ and, as shown above, to the concentration product $[Hg^{2+}] \cdot [\text{by-product}]$. This should therefore be constant at a given Fe^{2+} concentration. The results in Tables 1 and 2 show this to be so. It can also be seen from Table 2 that an increase of the Hg^{2+} concentration accelerated the feeding reaction and so produced a significant reduction of the feeding time and even its elimination, as well as less accumulation of the by-product.

However, when the initial concentration of Fe^{2+} was increased, the time of the feeding stage remained almost constant (Table 3). This result arose because the iron plays different roles. As a reagent of Reactions R1 and R2, it accelerates the feeding, but by sequestering Hg_c^0, it removes the catalyst and also delays Reaction R3. These two opposite effects compensate each other, making the time of feeding very similar. This result demonstrates the high degree of deadening of the system. In Table 3, the by-product absorbance cannot be used as reference point for the concentration of Hg_c^0 since the colour depends on the Fe^{2+} concentration which is variable here.

3.7. The hump

When Reaction A was slow, as in the range of 0.5–5.0 mM of each reagent, the kinetic curve showed another interesting feature: the initially large slope of

Table 3

Effect of Fe^{2+} concentration on the feeding stage and on the concentration of the by-product

The Hg^{2+} concentration was 10 mM, and the temperature 45°C.

Fe^{2+} (mM)	Feeding rate (A/min)	Feeding time (min)	Maximum absorbance at 450 nm
25	0.011	33	0.01
50	0.032	35	0.10
100	0.054	37	0.40

Table 2

Effect of Hg^{2+} concentration on the feeding time

The Fe^{2+} concentration was the same (50 mM) for all cases, and temperature was 45°C throughout.

Hg^{2+} (mM)	Feeding time (min)	Maximum by-product absorbance[a]	Critical mass $[Hg^{2+}] \cdot [\text{by-product}]$[a]
25	95	1.089	27.2
50	50	0.595	29.7
100	0	0.283	28.3

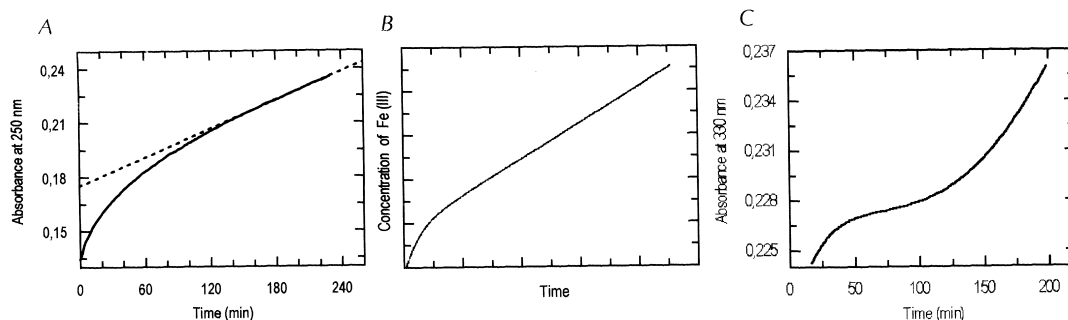[a]The maximum absorbance of the by-product at 450 nm was taken as its concentration.

Fig. 10. Hump at the beginning of the progress curve. (A) Hump followed by the lengthy linear progress of the feeding phase in Reaction A with 0.5 mM Hg^{2+} and 1 mM Fe^{2+} at 80°C. (B) The same effect reproduced with the computer program *Mercury*. (C) Hump before the surface autocatalysis in Reaction B with 25 mM Hg_2^{2+} and 50 mM Fe^{2+} at 35°C. The low temperature slowed the reaction down allowing the appearance of the hump.

the absorbance–time curve decreased very soon after starting, forming a hump before the long feeding stage (Fig. 10A). This behaviour could be reproduced in the computer simulation by using a value of k_3 which was much smaller than k_2 (Fig. 10B). This hump could also be seen in Reaction B under conditions of slow running (e.g., at low temperature). Unlike Reaction A, Reaction B was activated immediately after the hump without the subsequent linear behaviour (Fig. 10C). This result shows that the feeding stage can only occur when Hg^+ is produced very slowly, as happens in Reaction A.

3.8. Variation of temperature

The effect of temperature on the reaction was investigated in the range between 20°C and 90°C. As

seen in Fig. 11A, raising the temperature greatly reduced the time needed for Reaction A to finish: e.g., with 50 mM of each reagent, the reaction took ca. 1 week at 20°C and 45 min at 60°C. A higher temperature produced a smaller accumulation of the by-product, a shorter induction period and a steeper autocatalytic rise, similar to the behaviour observed at a high Hg^{2+}/Fe^{2+} ratio (compare Figs. 2A and 11B). This indicates that Reaction R3 is more sensitive to temperature changes than Reaction R4.

3.9. Comparison with Adamson's work

The reaction orders during the induction period of Reaction A were found to be approximately 1 for Fe^{2+} and 3/2 for Hg^{2+}. The unusual reaction order for Hg^{2+} is a consequence of the complicated mech-
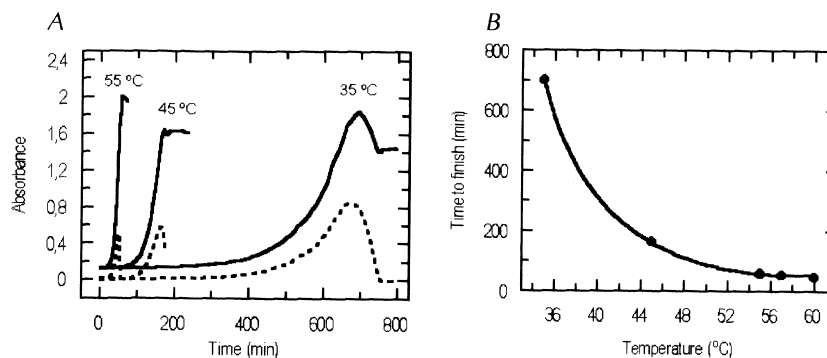

Fig. 11. Effect of temperature on the reaction rate. (A) Kinetic curves of experiments with 50 mM Hg^{2+} and 50 mM Fe^{2+}. Full lines: Fe^{3+} recorded at 330 nm; dashed lines: the by-product recorded at 450 nm. (B) Effect of temperature on the time for the reaction to finish.

anism. The energy of activation determined for this stage was found to be 65.2 kJ mol^{-1}. The student in the second short report of Adamson [2] had obtained second order rate constants equivalent to half-lives of several years, as well as an activation energy of 64.8 kJ mol^{-1} which agrees surprisingly well with our own value. This strongly suggests that his readings had only been taken during the very slow induction period. The far shorter half-life of several days quoted by Adamson [1] earlier is therefore likely to have been based on runs which had included the fast autocatalytic stage. This would explain the curious discrepancy in the literature. The discovery of the formation of colloidal mercury also resolves the disagreement between Adamson and earlier workers as to the products of the reaction.

4. Conclusions

The results of the laboratory experiments and the computer simulations lead to the following conclusions.

(1) Both Reactions A and B exhibit unusual and strong autocatalysis. For this to happen, the concentration ratio Hg^{2+}/Fe^{2+} in Reaction A as well as the temperature must be moderately high. According to the proposed model, this catalysis arises because Reaction R2 consumes 1 mol Hg^+ while Reaction R3 produces 2 mol Hg^+, thus promoting a chain reaction.

(2) The autocatalysis in Reaction A is preceded by a lengthy slow induction or feeding stage where the system is in a quasi-steady state. The autocatalysis starts when a given critical mass of the product $[Hg^{2+}]\cdot[Hg_c^0]$ is reached. A high Hg^{2+}/Fe^{2+} ratio shortens the feeding stage, and the same effect is achieved by increasing the temperature.

(3) Both Reactions A and B produce colloids of metallic mercury, as demonstrated by the Tyndall effect and electrophoresis. This colloid is present in two different forms, a yellow-green form (the by-product) and a colourless one. As the reaction proceeds, the by-product is accumulated. With similar initial concentrations of Hg^{2+} and Fe^{2+} in Reaction A, the by-product disappears at the end of the reaction, but with a low Hg^{2+}/Fe^{2+} concentration ratio, it remains. In general, a high Fe^{2+} concentration favours the accumulation of the by-product. Both forms of the colloid are stabilised by positive charges. Further research should be carried out to study this interesting reaction system in more detail.

Appendix A

Values of the parameters and initial conditions for the reaction between Fe^{2+} and Hg^{2+} (Reaction A) simulated by computer which gave the results presented in Fig. 8. The real values of the rate constants may different from these because similar curves could be produced by simultaneously varying several of the parameters. Further work will explore this.

Extinction coefficient of Fe^{+3} at 330 nm: 18.5 M^{-1} cm^{-1}.

Initial concentrations
$Fe^{2+} = 0.05$ M
$Hg^{2+} = 0.05$ M

Rate constants
$K_1 = 1.42 \times 10^{-7}$ M^{-1} s^{-1}
$K_{-1} = 10^{-10}$ M^{-1} s^{-1}
$K_2 = 1.67 \times 10^{-4}$ M^{-1} s^{-1}
$K_{-2} = 10^{-6}$ M^{-1} s^{-1}
$K_3 = 6.67 \times 10^{-5}$ M^{-1} s^{-1}
$K_{-3} = 10^{-6}$ M^{-1} s^{-1}
$K_4 = 1.67 \times 10^{-5}$ M^{-1} s^{-1}
$K_{-41} = 3.3 \times 10^{-6}$ s^{-1}
$K_{-42} = 1.67 \times 10^{-3}$ s^{-1}
$K_5 = 1.67 \times 10^{-4}$ M^{-1} s^{-1}
$K_{-5} = 1.67 \times 10^{-9}$ s^{-1}

References

[1] A.W. Adamson, J. Phys. Chem. 56 (1952) 858.

[2] A.W. Adamson, Discuss. Faraday Soc. 29 (1960) 125.

[3] Gmelins Handbuch der Anorganischen Chemie, 8th edn., System No. 34, Part A, Section 2, Verlag Chemie, Weinheim, 1962, p. 854.

[4] R.H. Betts, F.S. Dainton, J. Am. Chem. Soc. 75 (1953) 5721.

[5] G. Svehla, in: Vogel's Qualitative Inorganic Analysis, 6th edn., Longman, London, 1979, p. 57.

[6] J.A. Babor, J. Ibarz Aznárez, in: Química General Moderna, Marin, Barcelona, 1979, p. 746.

[7] E. Rabinowitch, Rev. Mod. Phys. 14 (1942) 112.

[8] M. Faraggi, A. Amozig, Int. J. Radiat. Phys. Chem. 4 (1972) 353.

[9] Gmelins Handbuch der Anorganischen Chemie, 8th edn., System No. 34, Section 1, Verlag Chemie, Weinheim, 1960, p. 222.

[10] Gmelins Handbuch der Anorganischen Chemie, 8th edn., System No. 34, Part A, Section 2, Verlag Chemie, Weinheim, 1962, p. 828.

[11] M. Spiro, Catal. Today 17 (1993) 517.

[12] P.L. Freund, M. Spiro, J. Phys. Chem. 89 (1985) 1074.

[13] D.J. Shaw, Introduction to Colloid and Surface Chemistry, 4th edn., Butterworth, Oxford, 1992.

[14] J.I. Steinfeld, J.S. Francisco, W.l. Hase, in: Chemical Kinetics and Dynamics, Prentice-Hall, Englewood Cliffs, NJ, 1989, p. 182.

[15] J.C. Nuño, I. Sánchez-Valdenebro, C. Pérez-Iratxeta, E. Meléndez-Hevia, F. Montero, Biochem. J. 324 (1997) 103.

[16] Microsoft QuickBASIC Version 4.5, for IBM PC, Microsoft, Redmond, Washington.

[17] H. Kacser, in: D.D. Davies (Ed.), The Biochemistry of Plants, Academic Press, San Diego, 1987. p. 38.